Far-field sound field estimation using robotized measurements and the boundary elements method

Caroline Pascal, Pierre Marchand, Alexandre Chapoutot, Olivier Doaré

25-29 August 2024
inter.noise
NANTES FRANCE

Far-field sound field estimation using robotized measurements and the boundary elements method

Caroline Pascal[1]
UME and U2IS, ENSTA Paris, Institut Polytechnique de Paris
828 Boulevard des Maréchaux, 91120 Palaiseau, France

Pierre Marchand[2]
POEMS, CNRS, Inria, ENSTA Paris, Institut Polytechnique de Paris
828 Boulevard des Maréchaux, 91120 Palaiseau, France

Alexandre Chapoutot[3]
U2IS, ENSTA Paris, Institut Polytechnique de Paris
828 Boulevard des Maréchaux, 91120 Palaiseau, France

Olivier Doaré[4]
UME, ENSTA Paris, Institut Polytechnique de Paris
828 Boulevard des Maréchaux, 91120 Palaiseau, France

ABSTRACT

Sound Field Estimation (SFE) is a numerical technique widely used to identify and reconstruct the acoustic fields radiated by unknown structures. In particular, SFE proves to be useful when data is only available close to the source, but information in the whole space is required. However, the practical implementation of this method is still hindered by two major drawbacks: the lack of efficient implementation of existing numerical methodologies, and the time-consuming and tedious roll-out of acoustic measurements. This paper aims to provide a solution to both issues. First, the measurements step is fully automated by using a robotic arm, able to accurately gather geometric and acoustic data without any human assistance. In this matter, a particular attention has been paid to the impact of the robot on the acoustic pressure measurements. The sound field prediction is then tackled using the Boundary Element Method (BEM), and implemented using the FreeFEM++ BEM library. Numerically simulated measurements have allowed us to assess the method accuracy, and the overall solution has been successfully tested using actual robotized measurements of an unknown loudspeaker.

1. INTRODUCTION

In experimental acoustics, it is a typical task to recreate the acoustic pressure field radiated by an arbitrary source using only a few microphone measurements. Specifically, *Sound Field Estimation*

[1]caroline.pascal.2020@ensta-paris.fr

[2]pierre.marchand@inria.fr

[3]alexandre.chapoutot@ensta-paris.fr

[4]olivier.doare@ensta-paris.fr

(SFE) seeks to use near-field measurements to accurately estimate an investigated source's far-field features. By doing so, it is possible to study the impact of the source in its environment, with no requirement for extensive and wide range measurements at a large distance from the source. The applicability of this approach has been demonstrated for the characterization of loudspeakers [1], as well as for the investigation of other noise sources, including airplanes [2], unmanned aerial vehicles [3], automobiles [4, 5], etc.

The foundations of SFE rely on two main aspects: the practical acoustic measurements, and the reconstruction method.

Acoustic measurements Performing a significant number of precisely positioned, near-field measurements is one of the primary difficulties faced when doing SFE acoustic measurements.

Traditionally, microphone arrays [3–5] have been used to address this problem, but their lack of flexibility, high cost and calibration requirements have led to the development of alternative solutions. For instance, actuated microphone arrays [2, 6, 7] have been introduced, allowing for variable resolution and large-scale measurements. Recent work also proposed to combine motion tracking [8] and localization techniques [9] with acoustic measurements, so that the microphone position is continuously monitored during the acquisition.

Eventually, the use of robots for acoustic measurements has been considered with, for instance, the robotized solution proposed by Klippel [1], using a cylindrical 3 d.o.f. robot. Yet, the use of robotic arms in acoustics still remains scarce, with few applications in non-destructive testing [10], room acoustics [11], and acoustic holography [12]. Furthermore, most of these procedures still limit themselves to planar measurements, hence not taking advantage of the robot maneuverability and autonomy, while the actual impact of the robot on the measurements remains to be studied.

Sound field estimation As for most reconstruction problems, SFE relies on two major steps: *modeling* and *identification*.

The modeling step focuses on the formal representation of the reconstructed sound field, and has been tackled in two major ways in the literature. The sound field may either be written as a finite weighted sum of elementary solutions of Helmholtz equation, or found as a solution of this equation, identified over a given function space.

The first option was initially dealt with a Fourier series approach [13], and has been subsequently improved to cope with aliasing issues [14]. Alternative methods opted for spheroidal elementary solutions as their expansion set [15], or considered punctual and distributed artificial sources to create it [16]. For instance, the spherical harmonics expansion [1] uses punctual acoustic sources, defined by a finite sum of spherical harmonics. In the end, all expansion based methods require (1) a clever choice of expansion set and (2) a discretization choice on this set, to ensure a good trade-off between reconstruction accuracy, computational resources and the risk of over-fitting. The identification of the expansion coefficients is usually performed with a least-square approach, often combined with a regularization term to ensure the stability of the reconstruction [17].

The second option, on the other hand, considered the direct resolution of Helmholtz equation, using an element-based approach. Considering the problem at stake, the *Boundary Elements Method* (BEM) received a particular interest [2, 8, 18]. BEM-based SFE provides more flexibility than the expansion approach as it only requires measurements to be performed on the nodes of a surfacic mesh. Specifically, the method remains unaffected by frequency aliasing, or by the placement of artificial sources, while the influence of the discretized function space choice can be predicted *a priori*. However, such flexibility comes at a cost, as computations are inherently more complex, and resource consuming.

More recently, following the emergence of learning-based methods in physics-based

problems, the use of convolutionnal neural networks [19] and physics informed neural networks [20] have also been considered, but remain limited by the need of a large amount of data, and the lack of physical guarantees on the reconstruction results.

Howbeit, despite their great diversity, these methods still remain scarcely implemented, and prove to be often hard to actually combine with custom measurements.

Problem statement and contributions At the crossing between time-consuming and tedious acoustic measurements, and the lack of efficient implementation of the existing SFE methodologies, we present a novel acoustic sound field estimation tool, handling both the measurements and reconstruction steps. The measurements are performed using a 6 d.o.f. robot, allowing for numerous and versatile measurements, and the reconstruction is performed using a optimized parallel implementation of BEM [21, 22]. Bearing in mind that the quality of a metrology system depends on the impact of each item in the acquisition chain, a recommended frequency range, as well as an expected reconstruction error are provided.

2. ACOUSTIC ROBOTIZED MEASUREMENTS

This section is dedicated to the presentation of our robotized acoustic measurements setup, along with the necessary hypothesis ensuring the measurements' validity.

2.1. Measurements setup

Drawing inspiration from previous works [11, 12, 23], the proposed setup (*c.f.* Figure 1) features

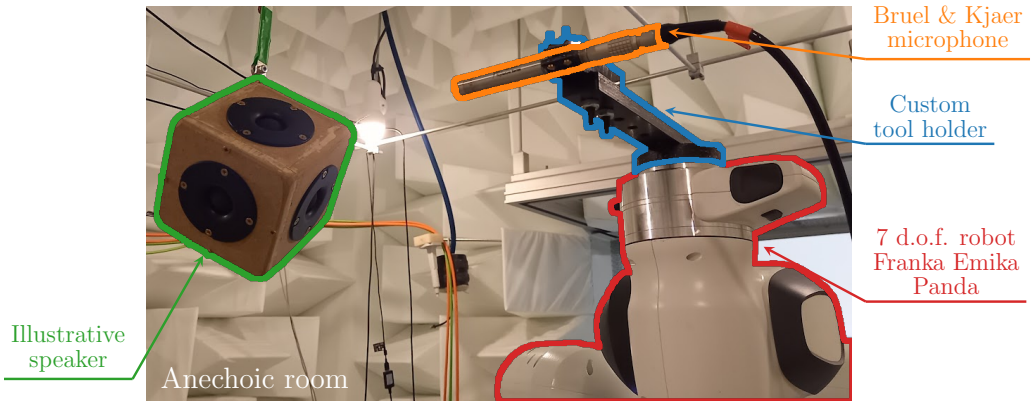

Figure 1: Robotized acoustic measurements setup.

a Franka Robotics Panda robot mounted in an anechoic chamber, and equipped with a custom microphone prop holding the sensor at a distance from the robot end-effector. The Moveit [24] stack available in ROS [25], has been chosen to handle the robot inverse kinematics and motion planning computation. This tool handfully bypasses the unpractical proprietary softwares and offers off-the-shelf tools for self and external collision avoidance.

On the sensor side, acoustic measurements are performed using the *measpy* [26] Python package, which ensures the synchronous dispatch and acquisition of signals through various classical sound cards and data acquisition systems.

All features are bundled up in a single ROS package *robot_arm_acoustics* [27], allowing to easily define the robotic cell collisions objects, and plan autonomous measurements routines along generic trajectories.

2.2. Robotized measurements validity hypothesis

The addition of a robot in an acoustic metrology setup inevitably introduces new sources of errors. To ensure that our installation still provides reliable measurements, three hypotheses are formulated and assessed.

Hypothesis 1: Time-invariant sound source The first constraint imposed by the robotized measurements setup is the sequential nature of the acquisitions. However, as our work focuses on the study of electro-acoustic devices, where the response to an input signal is measured, this lack of synchronicity is not a problem as long as the transfer function between these correlated signals is computed. From now on, all presented results will be derived from transfer functions computed using Welch's method [28], with a 10 s random noise input limited to the [10 Hz, 20 kHz] frequency range.

Additionally, the behavior of the studied sound source must remain the same throughout the whole characterization process, so that any measurement at a given location generates the same results, regardless to the time at which it was performed. As this hypothesis heavily relies on the studied object, it was experimentally assessed on a JBL Flip 2 loudspeaker, by performing a series of successive measurements at a fixed location.

As expected from an industrial product, the loudspeaker features a good time-invariability, with an average error of 0.25 dB over the audible frequency range.

Hypothesis 2: Low robot acoustic footprint The robot acoustic ego-noise and reflections are a major source of perturbations during the measurements. Even though parasitic noise generated by the robot can be filtered during the transfer function computation [28], the robot acoustic footprint is more complex to handle, as it depends on its spatial configuration and produces perturbations correlated to the input.

This hypothesis was first experimentally assessed by performing two successive series of measurements, with the microphone rigidly held in the same position. For the first series, the robot is moved aside, and for the second, it is placed as if it was holding the microphone. That way, the difference between the two series will only depend on the acoustic impact of the robot. The two-fold series of measurements were performed in six different robot configurations located around a JBL Flip 2, and the errors between the transfer functions obtained with and without the robot are displayed on Figure 2.

Unlike the time-invariability results, the robot acoustic footprint has a non-negligible impact on the quality of the measurements, especially at higher frequencies. Nevertheless, the deterioration caused by the robot induced reflections remain under an acceptable level for frequencies below $f = 1$ kHz, with an amplitude error below 2.25 dB and a phase difference of 0.25 rad at its maximum, as shown on Figure 2.

Hence, without further processing to separate the source from reflections, the frequency range [20 Hz, 1 kHz] should be considered as the validity frequency range for our robotized setup.

Hypothesis 3: Low robot positioning error The flawed positioning accuracy of robotic arms is often disregarded in metrology applications, even though sensor placement is of paramount importance in this context [2], especially when dealing with high frequency signals. In order to guard us against this pitfall, an extended calibration work has been carried out to ensure that the positioning accuracy of the Franka Robotics Panda used for our measurements remains lower than 2 mm, see [29] for more details.

If not completely removed, the actual impact of the remaining positioning errors on acoustic measurements will be considered negligible in the following.

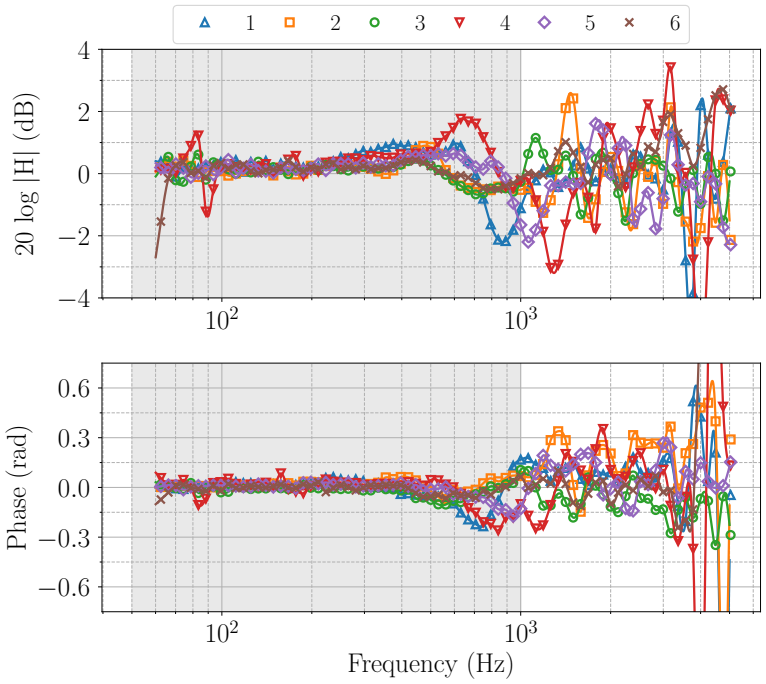

Figure 2: Robot acoustic footprint errors obtained for the six robot control configurations, relative to the robot-less transfer function. The shaded zone highlights the frequency range where the absolute value of the modulus error remains below 2.25 dB.

3. THE BOUNDARY ELEMENTS METHOD FOR SOUND FIELD ESTIMATION

The boundary elements method is a numerical method used to solve partial differential equations, that is particularly well suited for problems defined over an infinite domain [30], with boundary conditions defined on a closed surface. This boundary-wise approach made BEM a perfect candidate for the resolution of SFE problems [2, 8], but also hindered its practical use, as it requires measurements to be performed on a closed mesh surrounding the studied source. Luckily, the use of robotized measurements should conveniently ensure the reachability of the targeted mesh nodes.

Most BEM based SFE methods consider simple collocation techniques [2, 8], where the boundary integrals are computed by a point-wise approximation. We opted for the *Variational Boundary Element Method* (VBEM) approach [31], which describes both boundary surfaces and solutions space using higher order elements, leading to better reconstruction guarantees at the price of slightly lengthier computations. In the remainder of this section, the application of the VBEM to the SFE problem will be detailed with a particular focus on its theoretical reconstruction of errors estimates.

3.1. Problem statement and indirect resolution method

The SFE problem can be formulated as an exterior Dirichlet problem for Helmholtz equation such as a solution of the free-field acoustic equation in the infinite 3D space is searched for, knowing its value on a bounded surface. As pictured on Figure 3, let us denote by $\partial\Omega$ the surface on which the measurements are performed, and by Ω the exterior domain over which the complex sound field p is to be estimated. Denoting by G the Green function associated to Equation (1), we can define the well-posed [32] combined-layer potential C, as in [30]:

$$\forall u : \partial\Omega \to \mathbb{C},\ \forall x \in \mathbb{R}^3 \setminus \partial\Omega,\ C(u)(x) = \int_{\partial\Omega} \frac{\partial G(x,y)}{\partial \mathbf{n}_y} u(y) d\sigma(y) - ik \int_{\partial\Omega} G(x,y) u(y) d\sigma(y), \quad (2)$$

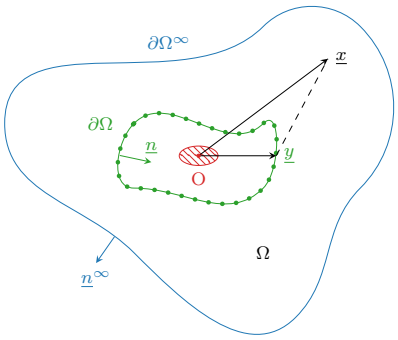

Helmholtz's equation.
Constant wave number $k \in \mathbb{R}$, harmonic hypothesis.

$$\begin{cases} \Delta p + k^2 p = 0 & \text{in } \Omega, \\ p = p_0 & \text{on } \partial\Omega, \\ \lim\limits_{\partial\Omega^\infty \to \infty} \left(\dfrac{\partial}{\partial |x|} - ik \right) p(x) = 0. \end{cases} \tag{1}$$

Figure 3: Dirichlet exterior problem for the Helmholtz equation.

where $d\sigma$ is the surface measure on $\partial\Omega$, and u is such that both integrals are well-defined.

It can be shown that this potential is an infinitely differentiable solution of Equation (1) on $\mathbb{R}^3 \setminus \partial\Omega$, which can be extended on $\partial\Omega$ provided that the value of u on $\partial\Omega$ is known, and such that the Dirichlet boundary conditions are satisfied. Introducing the Dirichlet trace operator on $\partial\Omega$, $\gamma_0^{\partial\Omega}$, this comes down to solve:

$$\text{Find } \; u : \partial\Omega \to \mathbb{C} \; \text{ s.t. } \; \gamma_0^{\partial\Omega} C(u) = \frac{u}{2} + C(u) = p_0. \tag{3}$$

Equation (3) defines a *Boundary Integral Equation* (BIE), which can be solved using a Galerkin variational approach, where the solution is sought in a finite dimensional subspace $V_h \subset H^{-1/2}(\partial\Omega)$. Even though the problem is well-posed, the resolution process is computationally expensive, as it requires the computation of singular integrals involving the Green function G evaluation on $\partial\Omega$, and the inversion of a fully-populated matrix.

Eventually, once the solution is found, the sound field can be reconstructed on the whole space in a straightforward way using the combined potential C from Equation (2).

3.2. Reconstruction error estimates

Despite being more complex, the variational resolution of the SFE problem comes with guarantees on the reconstruction error. In particular, J.C. Nedelec [33] focused on the case where the boundary surface $\partial\Omega$ is approximated by a mesh $\partial\Omega_h$ of size h and surface elements of order ℓ, and the solution approximated by Lagrange elements of order m. In this situation, and provided that kh remains small, it can be shown that the error between the actual solution p and its approximation p_h is such that:

$$\begin{aligned} \forall y \in \Omega, \; |p(y) - p_h(y)| \leq Ce(y, \partial\Omega) \Big[& ||p_0 - \tilde{p}_{0h}||_{L^2(\partial\Omega)} + \sqrt{h} ||p_0 - \tilde{p}_{0h}||_{H^{1/2}(\partial\Omega)} \\ & + h^{\ell+1} ||u||_{L^2(\partial\Omega)} + h^{m+2} ||u||_{H^{m+1}(\partial\Omega)} \Big], \end{aligned} \tag{4}$$

with $e(y, \partial\Omega)$ increasing with the distance between the point y and the boundary $\partial\Omega$, and Ψ describing the orthogonal projection of $\partial\Omega_h$ on $\partial\Omega$.

Hence, according to Equation (4), the reconstruction error will decrease as fast as $\mathcal{O}(h^{\min(\ell+1, m+2)})$, depending on the mesh and solution approximations. This result highlights the crucial impact of geometric approximation on the overall estimation error: if the surface is approximated by planar triangles, *i.e.*, $\ell = 1$, the estimation error will not decrease faster than $\mathcal{O}(h^2)$, regardless of the value of m.

3.3. Implementation and numerical simulations

As mentioned in previous section, the advantages and guarantees of BEM comes at the cost of complex and resource consuming boundary integral computations. However, benefiting

from the rise of high performance parallel computing, *FreeFEM++* [21] proposes a competitive implementation of the boundary element method and serves as a basis for our SFE tool. The related source code is also available in the *robot_arm_acoustics* ROS package [27], and offers clear interfaces as how to embed custom meshes and measurements.

Numerical simulations were then carried out in order to assess the agreement of our solution with the theoretically expected behaviors. The acoustic measurements are simulated using an acoustic monopole whose analytical pressure field expressions are sampled over a surrounding spherical mesh of varying size h and built with linear geometric elements. The BIE from Equation (2) is solved using P_0 Lagrange elements, and the reconstructed sound field estimated on a circular mesh of diameter 1 m, located in the $z = 0$ plane, and containing 100 nodes. The reconstruction error is then computed as the relative L^2 error between the exact and computed solutions on this mesh.

In our situation, the convergence rate of the computed solution towards the exact solution is theoretically expected to lay below $\mathcal{O}(h^2)$. This behavior was indeed confirmed by our numerical simulations, as shown on Figure 4, where the reconstruction error is plotted against the product of the mesh size h and the wave number k.

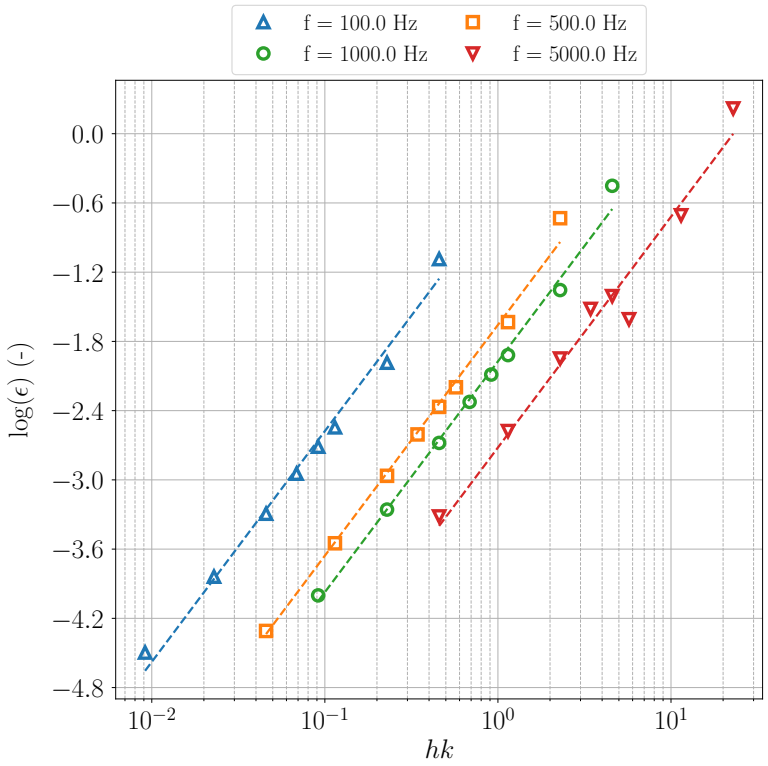

Figure 4: Reconstruction error obtained for measurements performed on a sphere of diameter 0.5 m, with increasing mesh sizes h. The dashed line represents the expected $\mathcal{O}(h^2)$ convergence rate.

It should still be mentioned that this trend seems to deteriorate at high frequencies when h increases, and that reconstruction errors quickly exceed 10 % as hk increases above 1. Enforcing this constraint, we fall back on the usual thumb rule of 6 measurements per wavelength often used in acoustic numerical simulations.

4. EXPERIMENTAL RESULTS

Bringing together our robotized measurements solution and SFE tool, this section describes how the complete procedure was applied to the acoustic characterization of an unmodeled JBL Flip 2

loudspeaker.

4.1. Experimental setup and Robotized measurements

Similarly to the previously described simulations, measurements were planned on a spherical mesh of size 0.025 m and diameter 0.35 m, centered around the loudspeaker. For the highest valid frequency identified in Section 2, hk remains below 1 at 1 kHz. The measurements were automatically performed by programming the robot to place the microphone successively at each face centroid, and align it with the local inward normal. Despite the large computation time allowed to the robot motion planning (more than 50 % of the total acquisition time), some poses remained unreachable due to collision avoidance. The missing measurements were recovered using an iterative hole-filling procedure, where each missing value is replaced by the averaged data of its neighbors.

An outlook of the post-processed measurements is displayed on Figure 5.

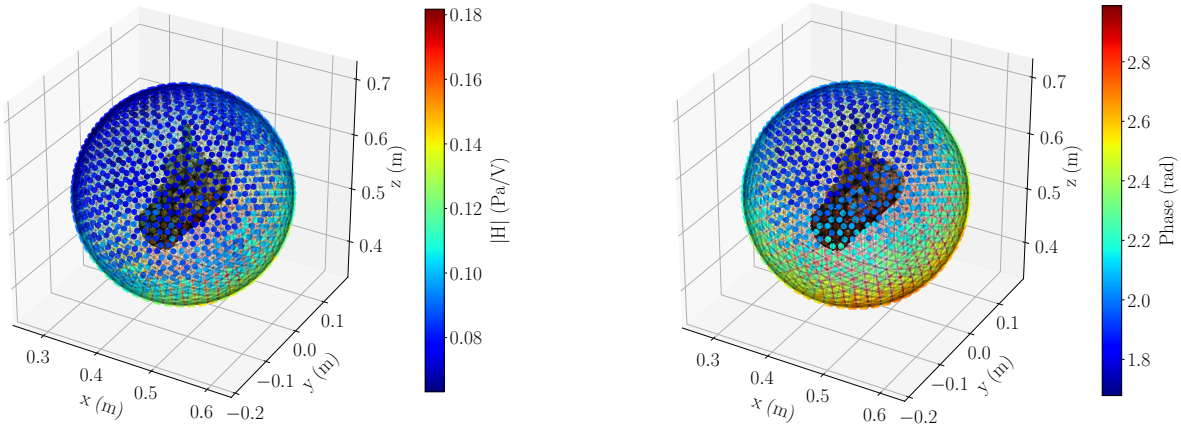

Figure 5: Example of post-processed measurements at $f = 500$ Hz. Left: modulus, Right: phase.

The acquisition was concluded by 20 additional verification measurements, located on a circular mesh of diameter 0.5 cm, lying in the horizontal $z = 0$ plane of the loudspeaker.

4.2. Sound field estimation results

Transferring the processed measurements to our BEM-based procedure, the sound field radiated by the loudspeaker was predicted on the verification circular mesh. A sample of the obtained results is shown on Figure 6, and the corresponding reconstruction error (*i.e.* the relative L^2 error computed on the verification mesh) are reported on Figure 7.

At first sight, the reconstruction seems to fit the measurements, with a faithfully rendering of the left monaural directivity pattern of the loudspeaker phase. However, a smoothing effect induced by SFE is clearly visible on both the modulus and phase reconstructions, especially in comparison with the more noisy verification measurements.

As was expected with measurements performed at a fixed distance form one another, *i.e.* with a linearly increasing hk as the frequency increases, the reconstruction error broadly increases with the frequency. For frequencies below 1 kHz, the reconstruction error globally remains below 15 %, but quickly rise to 30 % around 1 kHz, and towards 100 % when the validity frequency range is exceeded and hk exceeds 1. This sudden increase does not match the expected results of Equation (3), but seems to fit with the sharpening impact of the robot acoustic footprint at these frequencies (*c.f.* Figure 2), signaling a weakness in our hypothesis.

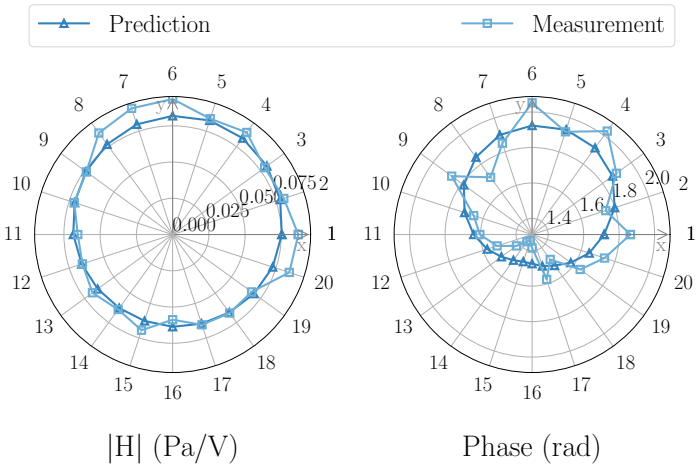

Figure 6: Predicted and measured acoustic pressure at $f = 500$ Hz. Left: modulus, Right: phase.

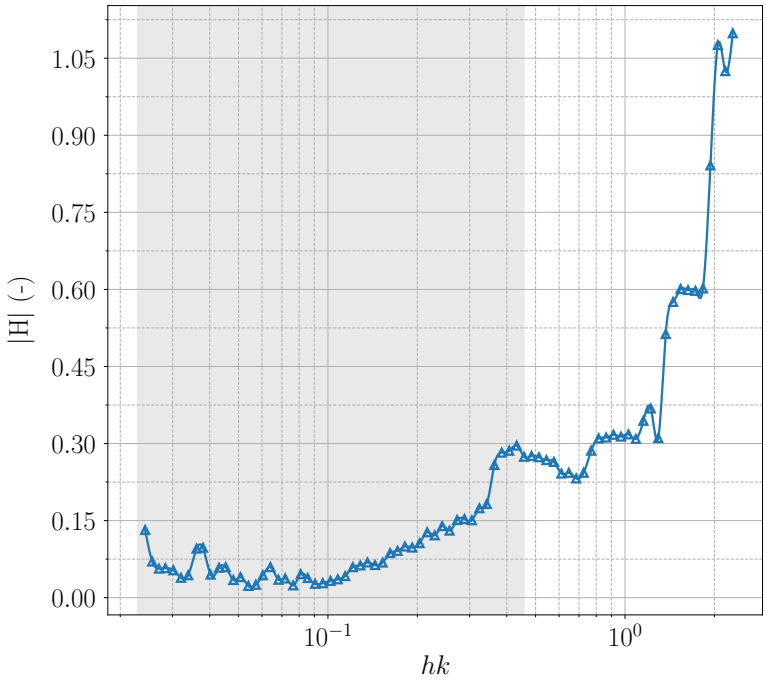

Figure 7: Reconstruction error obtained comparing the estimated acoustic pressure to the actual pressure measurements, with increasing frequency, *i.e.* increasing k. The shaded zone highlights the previously identified validity frequency range (*c.f.* Section 2).

5. CONCLUSIONS AND FUTURE WORK

Throughout this paper, we tackled the problem of sound field estimation considering both the measurements and reconstruction aspects. The requirements for spatially dense and versatile measurements were met using a robotic arm, which also allows for a fully automated acquisition of the data. The impact of the robot on the measurements was assessed, and found to be acceptable provided that the studied source is sufficiently repeatable, the robot properly calibrated, and the studied frequencies remain below 1 kHz. The reconstruction was performed using a resonance-free VBEM-based method, benefiting from *FreeFEM++* parallelisation capabilities. This approach was found to be computationally efficient, and to provide accurate results, as the expected reconstruction error decreases quadratically with the mesh size.

The overall procedure was finally tested on a JBL Flip 2 loudspeaker, and the estimated acoustic pressure was found to be in good agreement with the measured data, with a reconstruction error below 30 % for frequencies below 1 kHz.

Yet, the fast rise in the reconstruction error with the frequency highlighted weaknesses is our initial hypothesis and calls for a more cautious integration of the robot positioning inaccuracies, and filtering of its acoustic footprint. Among other leads, the gradient-based sound field separation might be considered for filtering the reflected sound waves [34].

The BEM implementation could also be improved, with the use of higher order elements, both geometric and algebraic, or the embedding of the trickier *Near-Field Holography* (NAH) problem, whose inverse-problem nature might help to reduce the observed smoothing effect.

ACKNOWLEDGEMENTS

Authors warmly thanks Thibault Toralba and Clément Yver, and Clément Savaro for their help setting up the robotized measurements setup.

This work was partially supported by Carnot TSN, Carnot Mines, and *Agence de l'Innovation de Défense* – AID – via *Centre Interdisciplinaire d'Études pour la Défense et la Sécurité* – CIEDS – (project 2022 - *Aéroacoustique des systèmes multi-PROpulseurs pour les drones* (APRO)).

REFERENCES

1. Wolfgang Klippel. Modeling and testing of loudspeakers used in sound-field control. In *Advances in Fundamental and Applied Research on Spatial Audio*. IntechOpen, February 2022.
2. Ferdy Martinus, David Herrin, Z. Tao, and Aandrew Seybert. Identification of aeroacoustic noise sources using inverse boundary element method. In *SAE 2005 Noise and Vibration Conference and Exhibition*, May 2005.
3. Hanwen Bi, Fei Ma, Thushara D. Abhayapala, and Prasanga N. Samarasinghe. Spherical array based drone noise measurements and modelling for drone noise reduction via propeller phase control. In *2021 IEEE Workshop on Applications of Signal Processing to Audio and Acoustics (WASPAA)*, pages 286–290, New Paltz, NY, USA, October 2021.
4. Sean F. Wu and Yuhua Wu. Reconstruction of radiated acoustic pressure fields from a complex vibrating structure. In *ASME 1998 International Mechanical Engineering Congress and Exposition*, pages 339–345. American Society of Mechanical Engineers Digital Collection, November 1998.
5. Svend Gade, Jesper Gomes, and Jørgen Hald. Using hand-held arrays for automotive nvh measurements. *Sound and Vibration*, 48:12–16, March 2014.
6. Maciej Szczodrak, Adam Kurowski, Józef Kotus, Andrzej Czyżewski, and Bożena Kostek. A system for acoustic field measurement employing cartesian robot. *Metrology and Measurement Systems*, 23(3):333–343, 2016.
7. Havard Vold, Parthiv Shah, Joshua Davis, Paul Bremner, Dennis McLaughlin, Philip Morris, Jeremy Veltin, and Richard McKinley. High resolution continuous scan acoustical holography applied to high-speed jet noise. In *16th AIAA/CEAS Aeroacoustics Conference*, Stockholm, Sweden, June 2010.
8. Zhong-Wei Luo, Daniel Fernandez Comesana, Chang-Jun Zheng, and Chuan-Xing Bi. A free field recovery technique based on the boundary element method and three-dimensional scanning measurements. *The Journal of the Acoustical Society of America*, 150(5):3929–3948, November 2021.
9. Dou Li, Haijun Wu, Yang Zha, and Weikang Jiang. A sound source reconstruction approach based on the machine vision and inverse patch transfer functions method. *Applied Acoustics*, 181:108180, October 2021.

10. Yannick Bernhardt, Dmitry Solodov, Dieter Müller, and Marc Kreutzbruck. Listening for airborne sound of damage: A new mode of diagnostic imaging. *Frontiers in Built Environment*, 6, 2020.
11. Mélanie Nolan, Samuel A. Verburg, Jonas Brunskog, and Efren Fernandez-Grande. Experimental characterization of the sound field in a reverberation room. *The Journal of the Acoustical Society of America*, 145(4):2237–2246, April 2019.
12. Nikola Knežević, Miloš Bjelić, and Kosta Jovanović. Automated sound intensity measurement with robot and intensity probe. *International Journal of Electrical Engineering and Computing*, 2(1):20–28, June 2018.
13. Julian D. Maynard, Earl G. Williams, and Y. Lee. Nearfield acoustic holography: I. theory of generalized holography and the development of nah. *The Journal of the Acoustical Society of America*, 78(4):1395–1413, October 1985.
14. Jørgen Hald. Basic theory and properties of statistically optimized near-field acoustical holography. *The Journal of the Acoustical Society of America*, 125(4):2105–2120, April 2009.
15. Sean F. Wu. On reconstruction of acoustic pressure fields using the helmholtz equation least squares method. *The Journal of the Acoustical Society of America*, 107(5):2511–2522, May 2000.
16. Nicolas P. Valdivia. Advanced equivalent source methodologies for near-field acoustic holography. *Journal of Sound and Vibration*, 438:66–82, January 2019.
17. Earl G. Williams. Regularization methods for near-field acoustical holography. *The Journal of the Acoustical Society of America*, 110(4):1976–1988, October 2001.
18. Mingsian R. Bai. Application of BEM (boundary element method)-based acoustic holography to radiation analysis of sound sources with arbitrarily shaped geometries. *The Journal of the Acoustical Society of America*, 92(1):533–549, July 1992.
19. Antonio Alguacil, Michaël Bauerheim, Marc C. Jacob, and Stéphane Moreau. Predicting the propagation of acoustic waves using deep convolutional neural networks. *Journal of Sound and Vibration*, 512:116285, November 2021.
20. Xingyu Chen, Fei Ma, Amy Bastine, Prasanga Samarasinghe, and Huiyuan Sun. Sound field estimation around a rigid sphere with physics-informed neural network. In *2023 Asia Pacific Signal and Information Processing Association Annual Summit and Conference (APSIPA ASC)*, pages 1984–1989, Taipei, Taiwan, October 2023.
21. Frédéric Hecht. New development in FreeFEM++. *Journal of Numerical Mathematics*, 20(3-4):251–265, 2012.
22. Pierre Marchand. *Schwarz Methods and Boundary Integral Equations*. Phd dissertation, Sorbonne Université, January 2020.
23. James Walker and Isak Worre Foged. Robotic methods in acoustics: Analysis and fabrication processes of sound scattering acoustic panels. In *36th eCAADe Conference*, volume 1, pages 835–840, Lodz, Poland, 2018.
24. David Coleman, Ioan A. Sucan, Sachin Chitta, and Nikolaus Correll. Reducing the barrier to entry of complex robotic software: A moveit! case study. *Journal on Software Engineering for Robotics*, 5(1):3–16, May 2014.
25. Morgan Quigley, Ken Conley, Brian Gerkey, Josh Faust, Tully Foote, Jeremy Leibs, Rob Wheeler, Andrew Y. Ng, et al. ROS: An open-source robot operating system. In *ICRA Workshop on Open Source Software*, volume 3, page 5, Kobe, Japan, May 2009.
26. Olivier Doaré. measpy. https://github.com/odoare/measpy, 2024.
27. Caroline Pascal. robot_arm_acoustic. https://gitlab.ensta.fr/pascal.2020/robot_arm_acoustic, 2024.

28. Peter Welch. The use of fast fourier transform for the estimation of power spectra: A method based on time averaging over short, modified periodograms. *IEEE Transactions on Audio and Electroacoustics*, 15(2):70–73, June 1967.
29. Caroline Pascal, Alexandre Chapoutot, and Olivier Doaré. A ROS-based kinematic calibration tool for serial robots. In *2023 IEEE/RSJ International Conference on Intelligent Robots and Systems (IROS)*, Detroit, MI, USA, October 2023.
30. Stefan A. Sauter and Christoph Schwab. *Boundary Element Methods*, volume 39 of *Springer Series in Computational Mathematics*. Springer, Berlin, Heidelberg, 2011.
31. Nicolas Valdivia and Earl Williams. Implicit methods of solution to integral formulations in boundary element method based nearfield acoustic holography. *Acoustical Society of America Journal*, 116:1559–1572, September 2004.
32. Simon N. Chandler-Wilde, Ivan G. Graham, Stephen Langdon, and Euan A. Spence. Numerical-asymptotic boundary integral methods in high-frequency acoustic scattering. *Acta Numerica*, 21:89–305, May 2012.
33. Jean-Claude Nedelec. Curved finite element methods for the solution of singular integral equations on surfaces in R3. *Computer Methods in Applied Mechanics and Engineering*, 8(1):61–80, 1976.
34. Zhong-Wei Luo, Chuan-Xing Bi, Yong-Bin Zhang, Xiao-Zheng Zhang, and Liang Xu. Reconstruction of the sound field radiated from a source in a noisy environment based on three-dimensional scanning measurements. In *48th International Congress on Noise Control Engineering (Inter-Noise 2019)*, volume 259, pages 1982–1989, Madrid, Spain, June 2019.